Received: 21 February 2018 | Revised: 7 April 2018 | Accepted: 12 April 2018

DOI: 10.1111/cas.13620

ORIGINAL ARTICLE

WILEY Cancer Science

Stromal immunoglobulin κC expression is associated with initiation of breast cancer in TA2 mice and human breast cancer

Shiwu Zhang[1] | Fei Fei[1,2] | Hua Wang[1] | Yanjun Gu[3] | Chunyuan Li[1,2] | Xinlu Wang[1,4] | Yongjie Zhao[5] | Yuwei Li[6]

[1]Department of Pathology, Tianjin Union Medical Center, Tianjin, China

[2]Nankai University School of Medicine, Nankai University, Tianjin, China

[3]Department of Pathology, Affiliated Hospital of Logistic University of People's Armed Police Force, Tianjin, China

[4]Graduate School, Tianjin University of Traditional Chinese Medicine, Tianjin, China

[5]Department of General Surgery, Tianjin Union Medical Center, Tianjin, China

[6]Departments of Colorectal Surgery, Tianjin Union Medical Center, Tianjin, China

Correspondence
Shiwu Zhang, Department of Pathology, Tianjin Union Medical Center, Tianjin, China.
Email: zhangshiwu666@aliyun.com.

Funding information
National Science Foundation of China (#81472729 and #81672426), the Foundation of Tianjin Health Bureau (15KG112) and the Foundation of Committee on Science and Technology of Tianjin (17YFZCSY00700 and 17ZXMFSY00120).

The initiation of spontaneous breast cancer (SBC) in Tientsin Albino 2 (TA2) mice is related to mouse mammary tumor virus (MMTV) infection, and MMTV amplification is hormonally regulated. To explore the insertion site of MMTVLTR in TA2 mouse genome, reverse PCR and nested PCR were used to amplify the unknown sequence on both sides of the MMTV-LTRSAG gene in SBC and normal breast tissue of TA2 mice. Furthermore, the clinicopathological significance of the insertion site was evaluated in 43 samples of normal breast tissue, 46 samples of breast cystic hyperplasia, 54 samples of ductal carcinoma in situ, 142 samples of primary breast cancer and 47 samples of lymph node metastatic breast cancer by RNA in situ hybridization. We confirmed that the insertion site of the MMTV-LTRSAG gene was located between Igκv2-112 and Igκv14-111 in chromosome 6 of TA2 mouse. IGκC was localized in the stromal cells of TA2 mouse with SBC and in human breast cancer tissues. Tumor cells were negative for IGκC in RNA in situ hybridization. The positive staining index of IGκC in stromal cells was the highest in lymph node metastatic breast cancer, followed by primary breast cancer, ductal carcinoma in situ, and breast cystic hyperplasia. Furthermore, the positive staining index of IGκC was related to the expression of ER, PR, HER2 and Ki-67. Our findings showed that stromal IGκC expression was associated with the initiation of SBC in TA2 mice. IGκC may be a high-risk factor for the initiation and progression of human breast cancer.

KEYWORDS
breast cancer, immunoglobulin κC, mouse mammary tumor virus, Tientsin Albino 2, triple negative breast cancer

1 | INTRODUCTION

Breast cancer is a very common type of cancer and a serious threat to women's health. Surgery accompanied with chemotherapy and targeted therapy is the most successful treatment strategy for breast cancer. However, 40% of patients die due to recurrence and metastasis.[1] The initiation of breast cancer is hormonally dependent. The mechanisms underlying hormone-regulated development of breast cancer are complicated and involve different pathways.[2-5] It has

Zhang and Fei equally contributed to the paper.

been reported that the human genome carries a number of distinct endogenous retroviral sequences that exhibit sequence similarity to MMTV. Wang et al[6] report that a 660-bp MMTV-like env gene sequence was found in approximately 38% of the sampled human breast cancer tissues but not in normal breast tissues or other tumors.

Tianjin Medical University established the spontaneous breast cancer (SBC) mouse model, TA2, following more than 50 years of research on this topic. The incidence of SBC in this model is more than 80%. The incidence of SBC was dependent on gravidity and frequency of pregnancy, and mouse mammary tumor virus (MMTV) infection.[7,8] MMTV is a retrovirus that is characterized by long terminal repeats (LTR). MMTV LTR-like sequences contain hormone-responsive elements (HRE), transcription enhancer factor-1 (TEF-1) family elements and an open reading frame (ORF) for superantigen (SAG).[6] Expression of the SAG gene, which is present in the provirus, is responsible for the production of SAG.[9] The MMTV promoter contains an HRE that can bind with progestin, glucocorticoid receptors and androgen receptors to promote the expression of MMTV genes.[10] Our previous studies confirmed that combined exogenous estradiol and progesterone treatment induces the initiation of breast cancer in TA2 mice without ovaries.[8] As a retrovirus, MMTV can integrate its genome into the mouse genome. When the virus DNA is inserted inside or even near an oncogene, it is able to change the expression of that gene, leading to development of cancer.[10] MMTV remains dormant until stimulated by hormones. The hormones bind to the repeat sequence, TGTTCT, in the HRE of MMTV-LTR. The incidence of SBC in TA2 mice is related to gravidity and frequency of pregnancy and MMTV infection. Estradiol and progesterone can bind to the HRE and subsequently induce the initiation of breast cancer.

The initiation of SBC in TA2 mice may be similar to that for the human pregnancy-associated breast cancer (PABC). PABC is defined as breast cancer diagnosed during pregnancy or within 1 year after delivery.[11,12] Breast cancer has a high incidence the first year after pregnancy. The mechanism underlying the development of PABC involves the hormonal changes during adolescence and pregnancy.[13] Furthermore, our previous studies have proved that SBC in TA2 mice is triple negative, which is an important subtype of invasive breast cancer with negative expression of the estrogen receptor (ER), progesterone receptor (PR) and HER2. Triple-negative breast cancer is more likely to affect younger women, and patients' prognosis is poor.

Based on the results of sequence analysis, we confirmed that the MMTV-LTR was integrated between immunoglobulin κv2-112 (IGκv2-112) and IGκv14-111 in chromosome 6 of the TA2 mice. IGκC RNA in situ hybridization showed that IGκC was expressed in the stromal cells of TA2 mice with SBC and in human breast cancer tissues. The positive staining index of IGκC was related to the development of human breast cancer and expression of ER, PR, HER2 and Ki-67. Tumor-infiltrating plasma cells were identified as the source of IGκC.[14] This study validated the prognostic value of IGκC in human breast cancer using RNA in situ hybridization in formalin-fixed, paraffin-embedded (FFPE) tissue.

2 | MATERIALS AND METHODS

2.1 | Spontaneous breast cancer tissue and normal breast tissue from TA2 mice

Spontaneous breast cancer appears in female TA2 mice with different frequency of pregnancy. The tumor tissues were removed after the mice were killed. Part of the tumor that did not undergo necrosis was frozen. Parts of the tumor from the mice with SBC and normal breast tissue were embedded in paraffin. H&E staining was used to confirm the diagnosis for SBC. These paraffin-embedded blocks were sectioned for RNA in situ hybridization. The Animal Ethics Committee of the National Research Institute approved the animal experimentation protocols and all animal experiments were performed according to guidelines (Guidelines for the Care and Use of Laboratory Animals) established by the Chinese Council on Animal Care.

2.2 | Reverse transcription PCR and sequence analysis

Total RNA from cells was isolated using TRizol (Invitrogen), and it was reverse-transcribed into cDNA according to the manufacturer's instructions (Tianjin Novcare Biotech). Aliquots of these cDNA samples were used for PCR. The level of MMTV-3′LTR expression was normalized to the level of GAPDH. The primer sequences for MMTV-3′LTR were 5′GACATGAAACAACAGGTACATGA3′ and 5′GGACTGTTGCAAGTTTACTC 3′ (full length 339 bp). The primer sequences for GAPDH gene were 5′ACCACAGTCCATGCCATCAC3′ and 5′TCCACCACCCTGTTGCTGTA3′ (full length 452 bp). Subsequently, the primer sequences of MMTV-LTRSAG gene (5′GTTG TTTCCCACCAAGGACGACCCGTCTGC3′, and 5′GGAGACGGG ATGGCGAACAGACACAAACAC3′, full length 1303 bp) were synthesized to amplify the total length of segments of MMTV-LTRSAG gene. Finally, we designed 2 pairs of PCR primers (primer 1: 5′GCTTATGTAAACCATGATATAAAAGAGTGC 3′, and 5′ATGCCAA GTTTGCAGCAGAGAATGAGTATG 3′, full length 3-4 kb; primer 2: 5′TATGTAAATGCTTATGTAAACCATG3′ and 5′CAGAGCTATGCCA AGTTTGCAGCAG3′, full length 3-4 kb) for reverse PCR and nest PCR, which were used to amplify the unknown sequence on both sides of the MMTV-LTRSAG gene. The sequence on both sides of MMTV-LTRSAG gene was analyzed by sequence similarity searching in NCBI-BLAST.

2.3 | Tissue sample

Paraffin-embedded human invasive breast cancer tissue samples were obtained from a patient group at the Department of Pathology at Tianjin Union Medical Center. The patient group comprised 140 women and 2 men, and the age range was 26-87 years, with the average age being 58.82 ± 11.69 years. None of the patients had been treated before the complete surgical removal of the tumor. Among these 142 cases of invasive breast cancer, 47 cases had lymph node metastasis and 54 cases had ductal carcinoma in situ, as

determined by pathological examination. Furthermore, out of these breast cancer samples, 46 cases were of breast cystic hyperplasia and 43 samples were normal breast tissue. The Hospital Review Board approved this study, and the confidentiality of patient information was maintained.

2.4 | Tissue microarray

In H&E staining sections, the typical lesions of primary invasive breast cancer, lymph node metastatic foci, ductal carcinoma in situ, cystic hyperplasia and normal breast tissue were marked and then located in the FFPE tissues. The tissues in which the cells did not undergo necrosis were chosen to make a tissue microarray with 1.5-mm cores (2.0 mm between cores). Two typical spots for each sample were chosen.

2.5 | RNA in situ hybridization in formalin-fixed, paraffin-embedded tissue

In situ hybridization was performed using a mouse RNAscope Probe-Mm-IGκC probe (catalog, 16356A, Advanced Cell Diagnostics [ACD]; Hayward, CA, USA) specific for IGκC, and the RNAscope 2.5 HD Reagent Kit- BROWN (catalog, 2002422, ACD) as directed by the manufacturer.[15,16] According to the factory instructions, the FFPE tissue microarray slides were deparaffinized and rehydrated. Endogenous peroxidase activity was inhibited before the slides were boiled in Pretreatment 2, followed by treatment with protease, and hybridization with the target oligo probes (ACD). After hybridization, a 6-step amplification process (preamplifier, signal enhancer, amplifier, label probe, signal amp and DAB-linked labeling) was performed. Finally, these slides were counterstained with hematoxylin. Specific in situ hybridization signals appeared as punctate brown spots. The RPE65 probe was used as a positive control, and the bacterial dapB probe was used as a negative control.

2.6 | Review and scoring of RNA in situ hybridization-stained tissue microarray sections

The positive staining of IGκC was confirmed by the observed punctate brown spots, and the stromal cells were positive for IGκC in situ hybridization staining. The tumor cells were negative for the staining. The percentage of positive cells per high-power field was evaluated visually, and the fields were stratified as follows: 0 (negative) for no positive cells, 1 (weak) for <10% positive cells, 2 (moderate) for 11%-30% positive cells, and 3 (strong) for >31% positive cells.

2.7 | Immunohistochemistry

Immunohistochemistry (IHC) was performed using an IHC autostainer (BenchMark, Roche, Arizona, USA). The 4-μm-thick sections were deparaffinized in EZprep, the endogenous peroxidase activity was inhibited with 3% hydrogen peroxide, and the sections were subjected to antigen retrieval in cell-conditioning solution (CC1) at 95°C for 30 minute. LCS was added on the sections to avoid evaporation, and the sections were incubated at 37°C for 1 hour with 100 μL ER (Kit-0012, ready-to-use), PR (MAB-0675, ready-to-use), HER2 (MAB-0198, ready-to-use) and Ki-67 (RMA-0731, ready-to-use) (all from MXB Biotechnologies, Fuzhou, China). Following incubation, a secondary antibody was added to the samples at 37°C for 15 minute, and the signal was detected using the chromogen 3,3′-diaminobenzidine. The nuclei were counterstained with hematoxylin.

2.8 | Evaluation and scoring of estrogen receptor, progesterone receptor, Ki-67 and HER2 immunohistochemical staining

Immunohistochemistry was conducted, and the proportion of the malignant cells staining positive for ER, PR, Ki-67 and HER2 was quantitatively measured using light microscopes. The percentage score is defined as the percentage of positively stained tumor cells among the total number of malignant cells assessed.[17] For ER and PR, samples with more than a 10% score were defined as positive.[18] For Ki-67, these samples were divided into 2 groups, 1 comprising of samples with an average cell percentage of >14%, and the other with a positive cell percentage of ≤14% (a cut-off of 15% for Ki-67 was defined according to the international recommendations).[19-22] For HER2, the basis of IHC scores (0, 1+, 2+, 3+) were used. Samples with IHC scores of 3+ and certain samples with a score of 2+ were defined as positive, and those with an IHC score of 0 and 1+, and certain samples with a score of 2+ were defined as negative. Samples with HER2 score 2+ were defined positive or negative based on the results of FISH, which can be used to prove the gene amplification.[23]

2.9 | Statistical analysis

Statistical software SPSS 17.0 statistical software (IBM Corporation, USA) was used to evaluate the data, and $P < .05$ was defined as statistically significant. Pearson's χ^2-test was used to analyze the differences in the IGκC staining index among different groups. A Mann-Whitney *U* test was used to analyze the differences of IGκC staining index between 2 groups.

3 | RESULTS

3.1 | Morphological characteristics of different breast lesions during the process of spontaneous breast cancer development

Normal breast tissue samples and samples from different breast lesions, including atypical hyperplasia, intraductal papilloma, ductal carcinoma in situ, invasive breast cancer, and metastatic breast cancer at different stages of development and progression of SBC in TA2 mice were analyzed. Five pairs of mammary glands were

assessed, and it was observed that all these different breast lesions could appear in 1 TA2 mouse. Figure 1A shows the morphologic characteristics of normal breast tissue (Figure 1Aa), atypical hyperplasia (Figure 1Ab) and invasive breast cancer (Figure 1Ac) from TA2 mice.

3.2 | MMTV-3′LTR sequences in the cDNA and genome of TA2 mice

The DNA and total RNA of SBC and normal breast tissue from TA2 mice were extracted from normal breast tissue and breast cancer tissue. Total RNA was reverse transcribed to cDNA. Based on the primer of MMTV-3′LTR, PCR was performed. The results of agarose gel electrophoresis of PCR products as observed by the gel imaging system indicated that MMTV-3′LTR sequences existed in the obtained cDNA (Figure 2Ba) and in the genome (Figure 2Bb) of TA2 mice.

3.3 | Integration of the MMTV-LTRSAG gene in the TA2 mouse genome and its amplification

Using the primer for the MMTV-LTRSAG gene, the PCR product, 1303 bp in length, was acquired. Figure 2Bc shows that the MMTV-LTRSAG gene was integrated into the genome of TA2 mice with breast cancer. Furthermore, 2 pairs of PCR primers were designed to amplify the unknown sequence on both sides of the MMTV-LTRSAG gene using reverse PCR and nest PCR (Figure 2Bd).

3.4 | Sequence of the unknown sequence on both sides of the MMTV-LTRSAG gene

The sequence lengths of forward and reverse PCR primers are 1090 and 1024 bp, respectively, and detailed information regarding them is provided in the Data S1. Using NCBI-BLAST, it was observed that the sequence of forward PCR primer did not match with that of

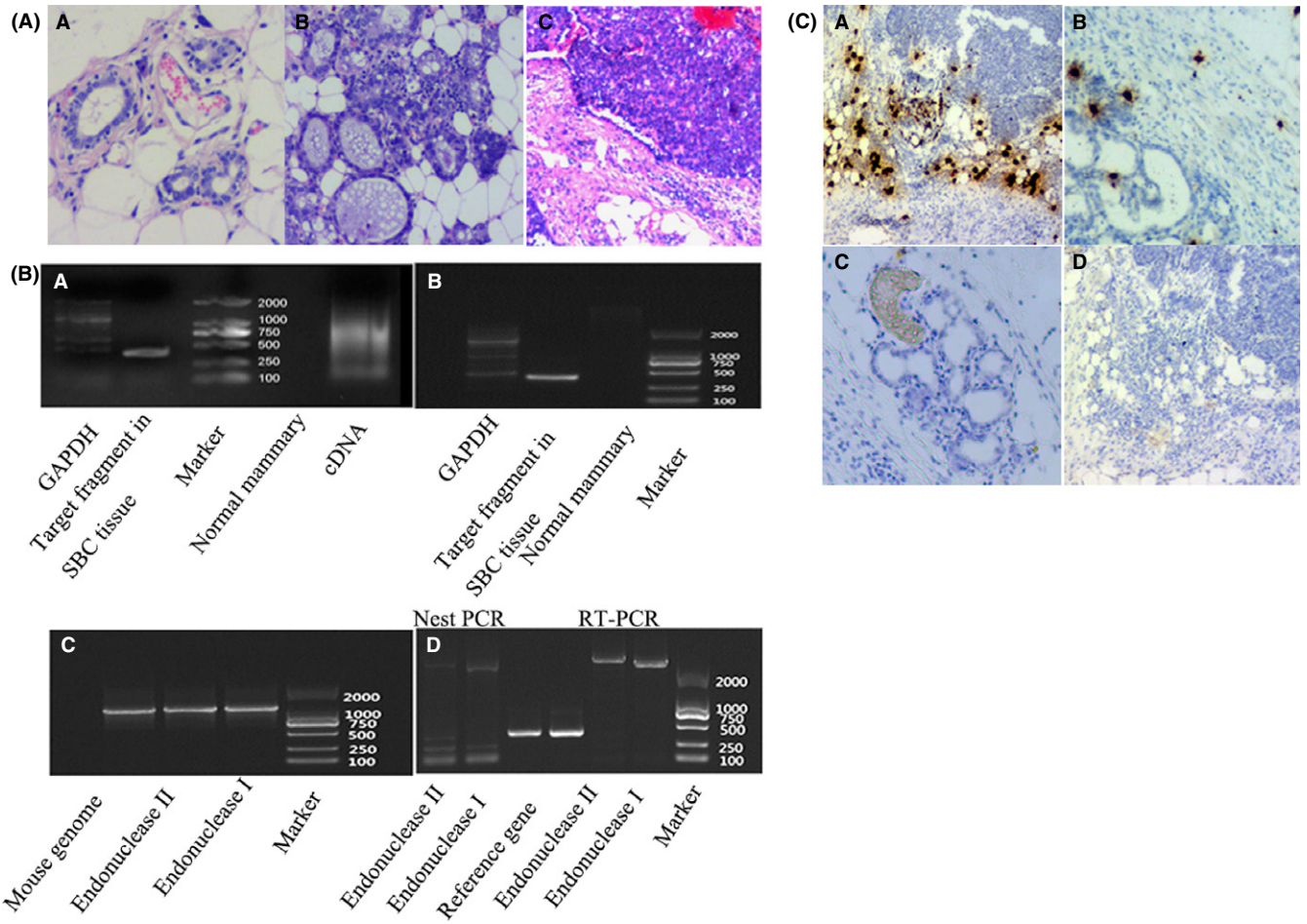

FIGURE 1 A, Morphological characteristics of different breast tissue in TA2 mice: (a) Normal breast tissue (H&E, ×100), (b) Hyperplasia of breast tissue (H&E, ×100) and (c) SBC (H&E, ×100). B, (a) Results of RT-PCR analysis of MMTV3′LTR from normal breast tissue and breast cancer, (b) results of MMTV3′LTR PCR in genome from normal breast tissue and breast cancer, (c) results of MMTV-LTRSAG PCR in TA2 mouse genome and (d) results of unknown sequence on both sides of the MMTV-LTRSAG gene based on reverse PCR and nested PCR. C, Stromal IgκC RNA in situ hybridization in TA2: (a) Strong staining of IgκC staining in SBC (×100), (b) weak staining of IgκC staining in hyperplasia breast tissue of TA2 with SBC (×100), (c) staining of IgκC^{-} normal breast tissue of TA2 with SBC (×100) and (d) negative control (×100)

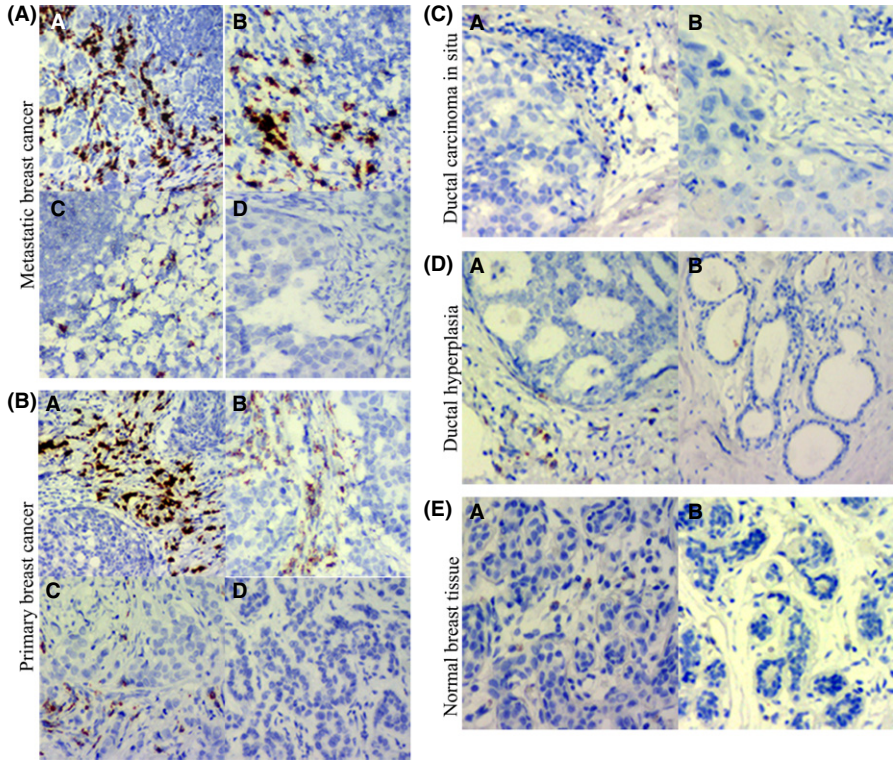

FIGURE 2 A, Stromal IgκC RNA in situ hybridization staining in lymph node metastatic breast cancer: (a) Strong staining of IgκC RNA (score 3) (×100), (b) moderate staining of IgκC RNA (score 2) (×100), (c) weak staining of IgκC RNA (score 1) (×100) and (d) negative staining of IgκC RNA (score 0) (×100). B, Stromal IgκC RNA in situ hybridization staining in primary breast cancer: (a) Strong staining of IgκC RNA (score 3) (×100), (b) moderate staining of IgκC RNA (score 2) (×100), (c) weak staining of IgκC RNA (score 1) (×100) and (d) negative staining of IgκC RNA (score 0) (×100). C, Stromal IgκC RNA in situ hybridization staining in ductal carcinoma in situ: (a) Weak staining of IgκC RNA (score 1) (×100), (b) negative staining of IgκC RNA (score 0) (×100). D, Stromal IgκC RNA in situ hybridization staining in atypical hyperplasia: (a) Weak staining of IgκC RNA (score 1) (×100) and (b) negative staining of IgκC RNA (score 0) (×100). E, Stromal IgκC RNA in situ hybridization staining in normal breast tissue: (a) weak staining of IgκC RNA (score 1) (×100) and (b) negative staining of IgκC RNA (score 0) (×100)

MMTV. However, the sequence similarity between the PCR product obtained using the forward PCR primer and the mice genome was more than 99%. Using NCBI-BLAST, it was also observed that the sequence of the PCR product obtained using the reverse PCR primer was part of the mice genome.

Results of PCR and sequence confirmed that MMTV-LRESAG was integrated into the mice genome. The 3′ terminal may connect with 2 sites, and both the sites were located in chromosome 6. One ID was ref|AC_000028.1| and ranged from 70364691 to 70365638, and the other ID was ref|NC_000072.6| and ranged from 68252138 to 68253085. Further analysis showed that the forward PCR primer sequence was located in the intergenic region between the upstream gene, IGκv2-112 (GeneID:38176), and the downstream gene, IGκv14-111 (GeneID:545847). Another 1120-bp-long forward PCR primer was sequenced (detailed information listed in the Data S1) and the sequence had 99% similarity with mouse IGκ. In addition, a 1103-bp-long reverse PCR primer sequence did not have any similarity with the mouse genome.

3.5 | IGκC RNA in situ hybridization in mouse tissue

As described above, different breast lesions were observed in 1 mouse. Breast cancer tissue, atypical hyperplasia tissue and normal breast tissue from 1 mouse were paraffin-embedded and used for RNA in situ hybridization. Results of IGκC RNA in situ hybridization showed that the stromal cells were positive. Strong staining of IgκC appeared in the breast cancer tissues of TA2 mice (Figure 1Ca). Weak staining of IgκC existed in the atypical hyperplasia tissue (Figure 1Cb), and normal breast tissue was negative for IgκC staining (Figure 1Cc). The negative control of bacterial dapB probe confirmed the reliability of the results (Figure 1Cd).

3.6 | Expression of IGκC was associated with the development of human breast cancer

The amplified sequence was identified, and its clinicopathological significance was evaluated by RNA in situ hybridization. IGκC staining intensities 3, 2, 1 and 0 can be observed in paraffin embedded tissue of 47 cases of lymph node metastatic breast cancer (Figure 2A), 142 cases of primary breast cancer (Figure 2B), 54 cases of ductal carcinoma in situ (Figure 2C), 46 cases of breast cystic hyperplasia (Figure 2D) and 43 cases without any disease (Figure 2E). IGκC was localized within the stroma, in between tumor cell nests. There was strong IGκC staining (score 3) in lymph node metastatic foci and primary breast cancer, and weak IGκC staining (score 1) in a few cases

of atypical hyperplasia and normal cases. The average positive rates of IGκC expression in normal breast tissue, breast cystic hyperplasia, ductal carcinoma in situ, primary breast cancer and lymph node metastatic breast cancer were 9.30%, 8.70%, 27.78%, 83.10% and 97.87%, respectively, and the differences among these groups were statistically significant ($\chi^2 = 173.317$, $P = .000$) (Table 1). The average staining index of IGκC in normal breast tissue, breast cystic hyperplasia, ductal carcinoma in situ, primary breast cancer and lymph node metastatic breast cancer were 0.09 ± 0.29, 0.08 ± 0.28, 0.28 ± 0.45, 1.23 ± 0.88 and 1.74 ± 0.89, respectively, and the differences among these groups were statistically significant ($\chi^2 = 173.385$, $P = .000$) (Table 2). Lymph node metastatic breast cancer presented the highest staining index of IGκC. The difference between ductal carcinoma in situ and normal breast tissue ($Z = -2.266$, $P = .023$), ductal carcinoma in situ and breast cystic hyperplasia ($Z = -2.412$, $P = .016$), ductal carcinoma in situ and primary breast cancer ($Z = -7.359$, $P = .000$), and primary breast cancer and lymph node metastatic breast cancer ($Z = -3.371$, $P = .001$) was statistically significant (Table 2).

3.7 | The expression of IGκC was associated with the expression state of estrogen receptor, progesterone receptor, HER2 and Ki-67 in primary human breast cancer

Estrogen receptor, progesterone receptor, HER2 and Ki-67 are routinely determined by IHC in human breast cancer. Among 142 cases of primary breast cancer, 126 cases had complete data for ER, PR, HER2 and Ki-67 immunohistochemical staining. Data for 16 cases were not available because the tissue samples were insufficient for performing all ER, PR, HER2 and Ki-67 immunohistochemical staining. According to the definition above, the primary invasive breast cancer samples were divided into 2 groups, ER/PR-positive and ER/PR-negative groups. The 126 cases of primary breast cancer comprised 87 cases with ER-positive samples (Figure 3Aa), 39 cases of ER-negative samples (Figure 3Ac), 60 cases with PR-positive samples (Figure 3Ba) and 66 cases with PR-negative samples (Figure 3Bc). The average positive index of IGκC RNA in situ hybridization in ER-positive (Figure 3Ab) and ER-negative samples (Figure 3Ad) was 1.07 ± 0.79 and 1.56 ± 1.02, respectively. The difference among them was statistically significant ($Z = -1.761$, $P = .006$). The average positive index of PR-positive (Figure 3Bb) and PR-negative samples (Figure 3Bd) were 1.02 ± 0.68 and 1.41 ± 1.02, respectively. The difference among them was statistically significant ($Z = -2.221$, $P = .001$). For Ki-67 immunohistochemical staining, these samples were also divided into 2 groups comprising 86 cases of average positive cell percentage >14% (Figure 3Ca), and 40 cases of average positive cell percentage ≤14% (Figure 3Cc). The average positive indexes of IGκC in Ki-67 with average positive cell percentage >14% (Figure 3Cb) and average positive cell percentage ≤14% (Figure 3Cd) were 1.44 ± 0.92 and 0.84 ± 0.68, respectively. The difference among them was statistically significant ($Z = -3.177$, $P = .001$). For HER2 immunohistochemical staining, these samples were also divided into 2 groups, HER2-positive and HER2-negative, based on the score. A total of 39 samples were HER2-positive, and 87 samples were HER2-negative (Figure 3Da-d). The average positive index of HER2-positive and HER2-negative groups was 1.53 ± 1.05 and 1.10 ± 0.80 (Figure 3De-h), and the difference between them was statistically significant ($Z = -2.133$, $P = .033$) (Table 3).

Based on the expression of ER, PR and HER2, 126 cases of primary breast cancer were divided into 4 groups: 66 cases were ER^+ or PR^+ and HER^-, 22 cases were ER^+ or PR^+ and HER^+, 17 were

TABLE 1 Differences of average positive rate of IGκC RNA in situ hybridization in different groups

	n	Average positive rate of IGKC RNA in situ hybridization	χ^2	P
Normal breast tissue	43	9.30% (4/43)[a]	173.317	.000
Breast cystic hyperplasia	46	8.70% (4/46)		
Ductal carcinoma in situ	54	27.78% (15/54)[b]		
Primary breast cancer	142	83.10% (118/142)		
Lymph-node metastatic breast cancer	39	97.87% (46/47)[c]		

[a]Comparison of ductal carcinoma in situ vs normal breast tissue, $\chi^2 = 8.791$, $P = .003$.
[b]Comparison of primary breast cancer vs ductal carcinoma in situ, $\chi^2 = 54.894$, $P = .000$.
[c]Comparison of lymph-node metastatic breast cancer vs primary breast cancer, $\chi^2 = 6.715$, $P = .010$.

TABLE 2 Differences in average positive rate of IGKC RNA in situ hybridization in different groups

	n	Average staining index of IGκC RNA in situ hybridization	χ^2	P
Normal breast tissue	43	0.09 ± 0.29[a]	173.385	.000
Breast cystic hyperplasia	46	0.08 ± 0.28[b]		
Ductal carcinoma in situ	54	0.28 ± 0.45		
Primary breast cancer	142	1.23 ± 0.88[c]		
Lymph-node metastatic breast cancer	47	1.74 ± 0.89[d]		

[a]Comparison of ductal carcinoma in situ vs normal breast tissue, $Z = -2.266$, $P = .023$.
[b]Comparison of ductal carcinoma in situ vs breast cystic hyperplasia, $Z = -2.412$, $P = .016$.
[c]Comparison of ductal carcinoma in situ vs primary breast cancer, $Z = -7.359$, $P = .000$.
[d]Comparison of primary breast cancer vs lymph-node metastatic breast cancer, $Z = -3.371$, $P = .001$.

ER^- or PR^- and HER^+, and 21 cases were ER^- or PR^- and HER^-. The average positive index of IGκC in ER^+ or PR^+ and HER^-, ER^+ or PR^+ and HER^+, ER^- or PR^- and HER^+, ER^- or PR^- and HER^- groups was 1.00 ± 0.78, 1.23 ± 0.81, 1.53 ± 1.12, and 1.70 ± 0.91. The difference among these 4 groups was statistically significant ($\chi^2 = 11.22$, $P = .011$). Furthermore, the average positive index of IGκC in the ER^- or PR^- and HER^- group was higher than that in the ER^+ or PR^+ and HER^- group ($Z = -3.070$, $P = .002$) (Table 4).

4 | DISCUSSION

The TA2 mouse model is ideal for breast cancer research. Even in the absence of any chemical stimulus, TA2 mice have a high incidence of SBC. The incidence of breast cancer in pregnant TA2 mice is up to 84.1%, and the incidence of breast cancer in male TA2 mice is only 1%.[7,24-26] Our previous studies have shown that the development of SBC is estradiol-dependent and progesterone-dependent. Estradiol and progesterone together induce replication of MMTV. High titer of MMTV induces carcinogenesis in mouse breast tissue.[7,8,27]

As described above, the initiation of SBC in TA2 mice was similar to that of human PABC because it was dependent on the gravidity and frequency of pregnancy. High levels of estradiol and progesterone during pregnancy can interact with the HRE in MMTV-LTR and promote MMTV amplification and SBC development in TA2 mice. MMTV LTR-like sequences have been detected in 41.5% of human breast cancers. There is evidence of poor prognosis in women with PABC diagnosed during pregnancy or within 2 years of delivery. Compared to nulliparous women, women with PABC, especially those diagnosed in the first year after delivery, presented a more advanced and aggressive stage of cancer and higher proportions of ER^-, PR^-, $HER2^+$ and triple-negative tumors.[11] Hormone receptor-negative cells were frequently observed in PABC patients compared to those in non-PABC patients.[28] PABC remains an understudied but important and growing clinical problem worldwide. The mechanisms underlying PABC occurrence and aggressiveness are incompletely understood.[29]

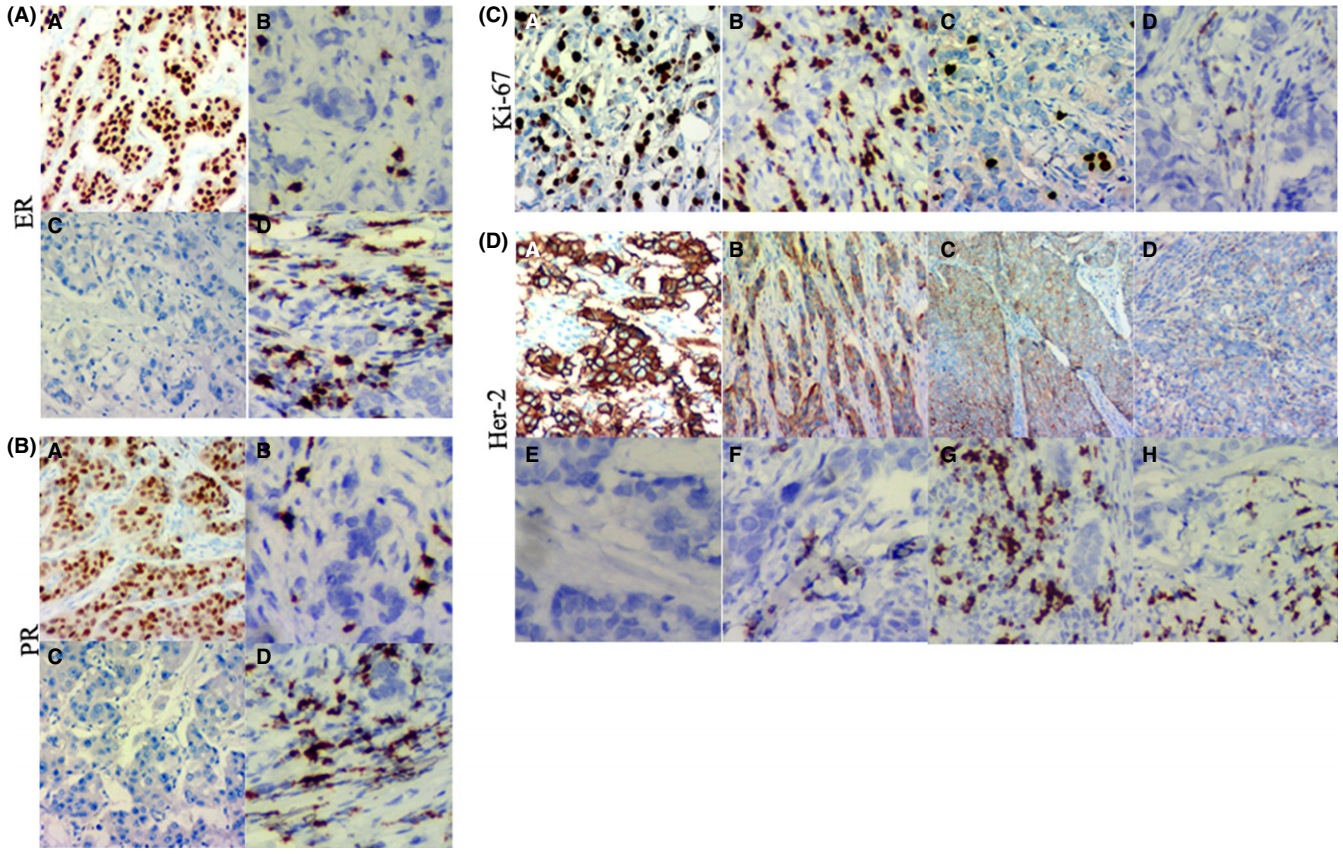

FIGURE 3 Immunohistochemical staining and stromal IgκC RNA in situ hybridization staining of human primary invasive breast cancer. A, (a) ER^+ (IHC ×200), (b) weak staining of IgκC RNA in ER^+, (c) ER^- (IHC ×200) and (d) strong staining of IgκC RNA in ER. B, (a) PR^+ (IHC ×200), (b) weak staining of IgκC RNA in PR^+, (c) PR^- (IHC ×200) and (d) strong staining of IgκC RNA in PR. C, (a) Ki-67 staining with more than 14% positive cell percentage (IHC ×200), (b) stong staining of IgκC RNA in (a), (c) Ki-67 staining with <14% positive cell percentage (IHC ×200) and (d) weak staining of IgκC RNA in (c). D, (a) Immunohistochemical staining of $HER2^+$ cells (score 3) (IHC ×100), (b) immunohistochemical staining of $HER2^-$ cells (score 2) (IHC ×100), (c) immunohistochemical staining of $HER2^-$ cells (score 1) (IHC ×100), (d) immunohistochemical staining of $HER2^-$ cells (score 0) (IHC ×100), (e) IgκC RNA staining of $HER2^+$ cells (score 3), (f) IgκC RNA staining of $HER2^-$ cells (score 2), (g) IgκC RNA staining of $HER2^-$ cells (score 1) and (h) IgκC RNA staining of $HER2^-$ cells (score 0)

TABLE 3 Differences of average positive rate of IGKC RNA in situ hybridization in relation to different expression of HER-2, ER, PR and Ki-67 in primary breast cancer cells

		n	Average positive index of IGKC RNA in situ hybridization	Z	P
HER-2	Positive	39	1.53 ± 1.05	−2.133	.033
	Negative	87	1.10 ± 0.80		
ER	Positive	87	1.07 ± 0.79	−1.761	.006
	Negative	39	1.56 ± 1.02		
PR	Positive	60	1.02 ± 0.68	−2.221	.001
	Negative	66	1.41 ± 1.02		
Ki-67	Positive cell percentage >14%	86	1.44 ± 0.92	−3.177	.001
	Positive cell percentage ≦14%	40	0.84 ± 0.68		

TABLE 4 Differences of average positive index of IGKC RNA in situ hybridization in relation to different phenotypes of primary breast cancer cells

	n	Average positive index of IGKC RNA in situ hybridization	χ^2	P
ER^+/PR^+ and HER^-	66	1.00 ± 0.78[a]	11.22	.011
ER^+/PR^+ and HER^+	22	1.23 ± 0.81		
ER^-/PR^- and HER^+	17	1.53 ± 1.12		
ER^-/PR^- and HER^-	21	1.70 ± 0.91		

[a]Comparison of ER/PR^+ and HER^- vs ER/PR^- and HER^-, $Z = -3.070$, $P = .002$.

Triple-negative breast cancer is the subtype of invasive breast cancer with ER^-, PR^- and $HER2^-$ phenotype. Triple-negative breast cancer is more likely to affect women of childbearing age, and it has a rapid progression and a poor prognosis. Women with triple-negative breast cancers have poorer survival than those with other breast cancers. Bauer et al compared 6370 cases of triple-negative breast cancer with 44 704 cases of other breast cancers in the USA. They found that the incidence of triple-negative breast cancer in women under 40 years of age was 1.53 times higher than that in women between the age of 60 and 69 years.[30] This phenotype of triple-negative breast cancer was significantly associated with shorter metastasis-free survival after undergoing adjuvant anthracycline treatment.

Pathological analysis showed that SBC is triple negative.[7,27] Furthermore, SBC has a high rate of metastasis to the lung and/or liver, and the rate of metastasis to the lung or liver exceeds 80%.[24,27] In this study, PCR and sequence analyses confirmed MMTV-3′LTR in SBC tissue from TA2 mice, but not in the normal breast tissue. The insertion site of the MMTV-LTRSAG gene was located between IGκv2-112 and IGκv14-111 in chromosome 6 of the mouse. IG has been assumed to be produced by B-cells or plasma cells. However, recent studies proved that that IG was expressed in many epithelial cancer cells, including breast, colon, lung, liver, cervical and oral cancers cells.[14,31,32] IG produced by non-hematopoietic cells show some unique characteristics. In particular, non-B-cell-derived IG is involved in cell survival and carcinogenesis.[31] It has been believed that immunoglobulin (Ig) can only be produced by B-cells or plasma cells. Recently, it was found that Ig was expressed in many epithelial cancer cells, including colon,[33] lung,[34] cervical[35] and oral[36] cancers. Wang et al[32] reported that IGκC was frequently expressed in acute myeloidleukemia cell lines and primary myeloblasts. Marcus Schmidt et al reported that IGκC expression was significantly associated with cell survival in paraffin-embedded tissues from 330 breast cancer patients. IGκC is localized within the desmoplastic stroma, in between tumor cell nests.[14] Identification of tumor-infiltrating plasma cells as the source of IGκC expression strongly suggests a role for humoral immunity in breast cancer progression.[37]

In this study, RNA in situ hybridization in FFPE samples showed that IGκC was localized in the stromal cells of breast cancer tissue of TA2 mice and humans. Tumor cells were negative for IGκC RNA in situ hybridization. Furthermore, to identify the clinicopathological significances of IGκC RNA expression and its association with different expression states of ER, PR, HER2 and Ki-67 in primary human breast cancer, the staining index of IGκC RNA in situ hybridization and ER, PR, HER2 and Ki-67 immunohistochemical staining was obtained. Lymph node metastatic breast cancer presented the highest IGκC staining index. In human primary invasive breast cancer, the positive staining index of IGκC was associated with $ER^-/PR^-/HER2^+$ and triple-negative tumors, and was similar to ER, PR and HER2 expression in PABC.

In summary, we provide evidence to prove that the MMTV-LTRSAG gene was integrated into the TA2 mouse genome and located between IGκv2-112 and IGκv14-111 in chromosome 6, and induced the initiation of SBC in TA2 mice, a triple-negative breast cancer with a high rate of metastasis to the lung and/or liver. IGκC expression in the stromal cells of breast cancer tissue was associated with the expression state of ER, PR, HER2 and Ki-67 in human invasive breast cancer cells. Further studies are required to analyze the molecular mechanisms underlying the amplification of IGκC RNA, the expression of IGκC, and, finally, the initiation of breast cancer through the expression of the MMTV-LTRSAG gene.

CONFLICT OF INTEREST

The authors have no conflicts of interest to declare.

ORCID

Shiwu Zhang http://orcid.org/0000-0002-5052-2283

REFERENCES

1. Kaufmann M, Rody A. Long-term risk of breast cancer recurrence: the need for extended adjuvant therapy. *J Cancer Res Clin Oncol*. 2005;131:487-494.
2. Demidov ON, Kek C, Shreeram S, et al. The role of the MKK6/p38 MAPK pathway in Wip1-dependent regulation of ErbB2-driven mammary gland tumorigenesis. *Oncogene*. 2007;26:2502-2506.
3. Gregorieff A, Clevers H. Wnt signaling in the intestinal epithelium: from endoderm to cancer. *Genes Dev*. 2005;19:877-890.
4. Iorio MV, Ferracin M, Liu CG, et al. MicroRNA gene expression deregulation in human breast cancer. *Cancer Res*. 2005;65:7065-7070.
5. Simin K, Wu H, Lu L, et al. pRb inactivation in mammary cells reveals common mechanisms for tumor initiation and progression in divergent epithelia. *PLoS Biol*. 2004;2:E22.
6. Wang Y, Jiang JD, Xu D, et al. A mouse mammary tumor virus-like long terminal repeat superantigen in human breast cancer. *Cancer Res*. 2004;64:4105-4111.
7. Sun B, Zhang S, Zhang D, et al. Clusterin is associated with spontaneous breast cancer in TA2 mice. *FEBS Lett*. 2007;581:3277-3282.
8. Yin Y, Yang Z, Zhang S. Combined treatment with exogenous estradiol and progesterone increases the incidence of breast cancer in TA2 mice without ovaries. *Cancer Lett*. 2011;311:171-176.
9. Golovkina TV, Dudley JP, Ross SR. B and T cells are required for mouse mammary tumor virus spread within the mammary gland. *J Immunol*. 1998;161:2375-2382.
10. Okeoma CM, Lovsin N, Peterlin BM, Ross SR. APOBEC3 inhibits mouse mammary tumour virus replication in vivo. *Nature*. 2007;445:927-930.
11. Johansson ALV, Andersson TM, Hsieh CC, et al. Tumor characteristics and prognosis in women with pregnancy-associated breast cancer. *Int J Cancer*. 2017;142:1343-1354.
12. Nargotra N, Kalita D. Pregnancy associated breast cancer: awareness is the key to diagnosis -a case report. *J Clin Diagn Res*. 2015;9:ED09-ED11.
13. Innes KE, Byers TE. First pregnancy characteristics and subsequent breast cancer risk among young women. *Int J Cancer*. 2004;112:306-311.
14. Schmidt M, Hellwig B, Hammad S, et al. A comprehensive analysis of human gene expression profiles identifies stromal immunoglobulin kappa C as a compatible prognostic marker in human solid tumors. *Clin Cancer Res*. 2012;18:2695-2703.
15. Wang F, Flanagan J, Su N, et al. RNAscope: a novel in situ RNA analysis platform for formalin-fixed, paraffin-embedded tissues. *J Mol Diagn*. 2012;14:22-29.
16. Smit-McBride Z, Oltjen SL, Radu RA, et al. Localization of complement factor H gene expression and protein distribution in the mouse outer retina. *Mol Vis*. 2015;21:110-123.
17. Urruticoechea A, Smith IE, Dowsett M. Proliferation marker Ki-67 in early breast cancer. *J Clin Oncol*. 2005;23:7212-7220.
18. Masuda H, Brewer TM, Liu DD, et al. Long-term treatment efficacy in primary inflammatory breast cancer by hormonal receptor- and HER2-defined subtypes. *Ann Oncol*. 2014;25:384-391.
19. Yerushalmi R, Woods R, Ravdin PM, Hayes MM, Gelmon KA. Ki67 in breast cancer: prognostic and predictive potential. *Lancet Oncol*. 2010;11:174-183.
20. Stuart-Harris R, Caldas C, Pinder SE, Pharoah P. Proliferation markers and survival in early breast cancer: a systematic review and meta-analysis of 85 studies in 32,825 patients. *Breast*. 2008;17:323-334.
21. de Azambuja E, Cardoso F, de Castro G Jr, et al. Ki-67 as prognostic marker in early breast cancer: a meta-analysis of published studies involving 12,155 patients. *Br J Cancer*. 2007;96:1504-1513.
22. Goldhirsch A, Wood WC, Coates AS, et al. Strategies for subtypes–dealing with the diversity of breast cancer: highlights of the St. Gallen International Expert Consensus on the Primary Therapy of Early Breast Cancer 2011. *Ann Oncol*. 2011;22:1736-1747.
23. Chenard MP, Wissler MP, Weingertner N, Mathelin C, Bellocq JP. HER2 gene and protein expression status of breast carcinoma can be reliably tested on a single slide. *Virchows Arch*. 2015;467:169-175.
24. Zhang D, Fei F, Li S, et al. The role of beta-catenin in the initiation and metastasis of TA2 mice spontaneous breast cancer. *J Cancer*. 2017;8:2114-2123.
25. Gu Y, Zhang S, Wu Q, et al. Differential expression of decorin, EGFR and cyclin D1 during mammary gland carcinogenesis in TA2 mice with spontaneous breast cancer. *J Exp Clin Cancer Res*. 2010;29:6.
26. Wang X, Huang C, Sun B, et al. The effect of high gravidity on the carcinogenesis of mammary gland in TA2 mice. *Am J Reprod Immunol*. 2010;63:396-409.
27. Sun B, Zhang S, Zhang D, et al. Identification of metastasis-related proteins and their clinical relevance to triple-negative human breast cancer. *Clin Cancer Res*. 2008;14:7050-7059.
28. Kim YG, Jeon YW, Ko BK, et al. Clinicopathologic characteristics of pregnancy-associated breast cancer: results of analysis of a nationwide breast cancer registry database. *J Breast Cancer*. 2017;20:264-269.
29. Ruiz R, Herrero C, Strasser-Weippl K, et al. Epidemiology and pathophysiology of pregnancy-associated breast cancer: a review. *Breast*. 2017;35:136-141.
30. Bauer KR, Brown M, Cress RD, Parise CA, Caggiano V. Descriptive analysis of estrogen receptor (ER)-negative, progesterone receptor (PR)-negative, and HER2-negative invasive breast cancer, the so-called triple-negative phenotype: a population-based study from the California cancer Registry. *Cancer*. 2007;109:1721-1728.
31. Martinet L, Garrido I, Filleron T, et al. Human solid tumors contain high endothelial venules: association with T- and B-lymphocyte infiltration and favorable prognosis in breast cancer. *Cancer Res*. 2011;71:5678-5687.
32. Wang C, Xia M, Sun X, et al. IGK with conserved IGKappaV/IGKappaJ repertoire is expressed in acute myeloid leukemia and promotes leukemic cell migration. *Oncotarget*. 2015;6:39062-39072.
33. Qiu X, Zhu X, Zhang L, et al. Human epithelial cancers secrete immunoglobulin g with unidentified specificity to promote growth and survival of tumor cells. *Cancer Res*. 2003;63:6488-6495.
34. Zheng H, Li M, Ren W, et al. Expression and secretion of immunoglobulin alpha heavy chain with diverse VDJ recombinations by human epithelial cancer cells. *Mol Immunol*. 2007;44:2221-2227.
35. Li M, Feng DY, Ren W, et al. Expression of immunoglobulin kappa light chain constant region in abnormal human cervical epithelial cells. *Int J Biochem Cell Biol*. 2004;36:2250-2257.
36. Zhu X, Li C, Sun X, et al. Immunoglobulin mRNA and protein expression in human oral epithelial tumor cells. *Appl Immunohistochem Mol Morphol*. 2008;16:232-238.
37. Pandey JP, Kistner-Griffin E, Black L, et al. IGKC and FcgammaR genotypes and humoral immunity to HER2 in breast cancer. *Immunobiology*. 2014;219:113-117.

SUPPORTING INFORMATION

Additional supporting information may be found online in the Supporting Information section at the end of the article.

How to cite this article: Zhang S, Fei F, Wang H, et al. Stromal immunoglobulin κC expression is associated with initiation of breast cancer in TA2 mice and human breast cancer. *Cancer Sci*. 2018;109:1825–1833. https://doi.org/10.1111/cas.13620